Modeling Hair Cell Tuning by Expression Gradients of Potassium Channel β Subunits

Krishnan Ramanathan and Paul A. Fuchs
The Center for Hearing and Balance, Department of Biomedical Engineering and Department of Otolaryngology, Head and Neck Surgery, Johns Hopkins University School of Medicine, Baltimore, Maryland 21205-2195 USA

ABSTRACT The receptor potential of sensory hair cells arises from the gating of mechanosensitive cation channels, but its amplitude and time course also depend on the number and kinetics of voltage-gated ion channels in each cell. Prominent among these are "BK" potassium channels encoded by the *slo* gene that support electrical tuning in some hair cells. Hair cells tuned to low frequencies have slowly gating BK channels, whereas those of higher-frequency hair cells gate more rapidly. Alternative splicing of the *slo* gene mRNA that encodes the pore-forming α subunit can alter BK channel kinetics, and gating is dramatically slowed by coexpression with modulatory β subunits. The effect of the β subunit is consistent with low-frequency tuning, and β mRNA is expressed at highest levels in the low frequency apex of the bird's auditory epithelium. How might an expression gradient of β subunits contribute to hair cell tuning? The present work uses a computational model of hair cell-tuning based on the functional properties of BK channels expressed from hair cell α and β *slo* cDNA. The model reveals that a limited tonotopic gradient could be achieved simply by altering the fraction of BK channels in each hair cell that are combined with β subunits. However, complete coverage of the tuning spectrum requires kinetic variants in addition to those modeled here.

INTRODUCTION

Some vertebrates use electrical tuning of sensory hair cells as a filtering mechanism to distinguish different frequencies of sound. The mechanism was first described in the turtle (Crawford and Fettiplace, 1980), and subsequently in amphibia, other reptiles, birds, and fish (Ashmore, 1983; Lewis and Hudspeth, 1983; Fuchs et al., 1988; Fuchs and Evans, 1988; Sugihara and Furukawa, 1989). Electrical tuning occurs by an interplay between voltage-gated calcium current and potassium current through neighboring large conductance, calcium and voltage-activated potassium (BK) channels (Lewis and Hudspeth, 1983; Art and Fettiplace, 1987; Hudspeth and Lewis, 1988a). Different electrical tuning frequencies result from the varied, cell-specific kinetics of the BK channels (Art and Fettiplace, 1987, Art et al., 1995; Hudspeth and Lewis, 1988b). Kinetically distinct BK channels may be formed by a combination of two mechanisms: alternative splicing of the *slo*-α gene that codes for the pore-forming BK channel subunit as well as modulation by accessory β subunits (Ramanathan et al., 1999, 2000; Jones et al., 1999). The present study examines the sufficiency of these mechanisms by incorporating the gating constants of cloned BK channels into a computational hair cell model.

The steady-state and kinetic properties of BK channels cloned from hair cells have been described previously by expression of the α (encoded by the *slo* gene) and β subunits in human embryonic kidney (HEK)293 cells (Ramanathan et al., 1999, 2000), as well as in oocytes (Jones et al., 1999). Certain alternatively spliced *slo*-α channels from the chick's cochlea (α_0 and α_{61}) have two- to threefold differences in deactivation kinetics as homomers, whereas combination with β subunits slows the kinetics of any α subtype substantially. Consistent with slowing of channel gating by β, in situ hybridization showed that the β mRNA is expressed at highest levels in hair cells at the apical (low frequency) end of the tonotopically organized sensory epithelium (Ramanathan et al., 1999).

These findings raised the suggestion that a smooth progression in hair cell-tuning frequencies might be achieved by "titration" with the modulatory β subunit. At least two possibilities can be imagined. Because BK channels are tetrameric structures, β subunits might combine progressively to generate as many as five classes of channel with intermediate kinetics from any one α subunit (subunit mixing). Alternatively, intermediate tuning frequencies may be achieved by mixing different ratios of α only and β-modified channels within each hair cell (channel mixing). This mechanism would be required if, for example, β subunits modulated BK gating in an all-or-none manner.

Earlier modeling efforts showed that the gating properties of native BK channels recorded from turtle hair cells could be used to reconstruct electrical tuning (Wu et al., 1995; Wu and Fettiplace, 1996). This model used subunit mixing to generate a population of five heteromeric channels whose graded expression generated the tonotopic array of tuned hair cells. The gating constants were taken from those of native BK channels of turtle hair cells, and did not explicitly test β subunit effects, which were unknown at the time. The present effort is also based on the turtle hair cell model. In contrast, we used gating constants from cloned and heterologously expressed BK channel subunits to test the possi-

Received for publication 4 May 2001 and in final form 9 October 2001.

Address reprint requests to: Paul Fuchs, Center for Hearing Science, Traylor Research Building, Room 521, Johns Hopkins University School of Medicine, Baltimore, MD 21205. Tel.: 410-955-6311; Fax: 410-614-4748; E-mail: pfuchs@bme.jhu.edu.

0006-3495/02/01/64/12 $2.00

bility that a continuum of tuning also can be produced simply by mixing two kinetically distinct channels in each cell, α-only and α-plus-β channels. That is, the gradient in β subunit expression simply alters the fraction of BK channels that are β-modified in each cell, a mechanism consistent with the all-or-none modulation of β subunits suggested by expression studies in *Xenopus* oocytes (Jones et al., 1999). This modeling effort demonstrates the ability of specific gene products to recreate electrical tuning equivalent to that based on the properties of native BK channels from hair cells, confirming that the α and β genes can be regulated to generate the tonotopic gradient. Further, the model shows that a gradient in tuning frequencies can result from even the simplest outcome of a β expression gradient (the varying mixture of only two channel types) despite substantial differences in kinetics of the individual channels. Finally, we have incorporated temperature effects on channel transition rates and conductance as well as on calcium diffusion parameters to account for tuning frequencies seen at the higher body temperature of the bird (Schermuly and Klinke, 1985; Fuchs and Evans, 1990).

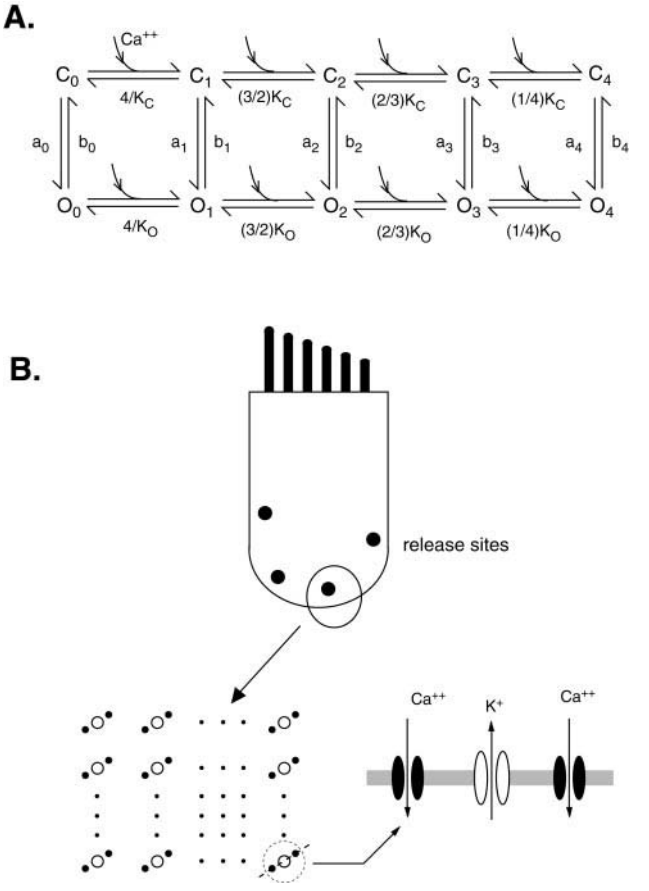

FIGURE 1 BK channel and hair cell models. (*A*) The allosteric (voltage-dependent MWC) scheme for BK channels has horizontal transitions that are calcium dependent and vertical transitions that are voltage dependent. The voltage-dependent MWC version assumes that each calcium-binding step has the same affinity. However, binding of calcium to the closed states may differ from the binding to the open states. The subscripts to the closed and open states indicate the number of calcium ions bound. Voltage-dependent gate movements between closed and open states are thought to occur allosterically with a single rate constant. a_x and b_x are the vertical transition rates that are dependent upon voltage. K_{CX} and K_{OX} are the dissociation constants for the binding of x^{th} calcium ion to the closed and open states respectively. (*B*) The hair cell model incorporates BK channels into functional units with two adjacent voltage-gated calcium channels. These are shown as clusters, as might occur at transmitter release active zones, but each BK channel is gated independently by its associated calcium channels. The number and kinetic properties of BK channels varies between model cells, but the ratio of two calcium channels to one BK channel remains constant, as do the gating properties of the voltage-gated calcium channels.

METHODS

Expression of BK channel genes in HEK293 cells

Two splice variants of the *slo* gene cloned from a chick's cochlear cDNA library were used in the present study. The pore-forming α subunits, α_0 and α_{61}, correspond to the original *cslo1* (Accession #U23821; Jiang et al., 1997), here called α_0, and to this cDNA with a 183 basepair insert at splice site 4 (α_{61}) as described previously (AF076268; Ramanathan et al., 2000). The variant exon α_{61} is closely related to the Strex exon described in adrenal chromaffin cells (Xie and McCobb, 1998; Xia et al., 1999). The *slo* β gene was cloned from quail papilla and shown to be identical to that first found in transformed fibroblasts (U67865; Oberst et al., 1997). A combination of α and β cDNAs, or single α cDNAs were transfected into HEK293 cells by calcium phosphate precipitation, as previously described (Ramanathan et al., 2000). Excised inside-out patches were formed from the transfected cells (detected by fluorescence of cotransfected GFP: "pGreen Lantern," Life Technologies, Carlsbad, CA). Voltage-clamp protocols to activate currents through BK channels in the presence of different concentrations of calcium were detailed previously (Ramanathan et al., 2000). For this study, it is sufficient to note that excised patches contained tens to hundreds of channels so that "macroscopic" currents were used for steady-state and kinetic fits. Also, β cDNA was added in a molar ratio of ~10:1 to that of the α subunit cDNA, in an effort to ensure a saturated effect on BK gating. Consistent with that expectation, α and β cotransfections produced homogeneous "β-altered" currents, with no indication that α-only channels coexisted with $\alpha\beta$ channels in cotransfected HEK cells.

Modeling BK channel gating

Steady-state parameters

Recordings from cloned and expressed BK channels were used to inform an allosteric gating model (also referred to as the voltage-dependent Monod-Wyman-Changeux (MWC) model) used previously to describe BK channel behavior (Cox et al., 1997; Cui et al., 1997). This model (Fig. 1 *A*) includes five closed states that interconvert to five open states in parallel through voltage-dependent transitions. Calcium binding moves the channels through adjacent closed or open states. Although this scheme oversimplifies BK gating behavior, it served to incorporate the kinetically distinct cloned channels into a hair cell model. Open probability was calculated from the conductance/voltage relation obtained from measurement of tail currents or steady-state currents normalized by driving force. Assuming independence of voltage gating and calcium binding, the equilibrium open probability of the allosteric gating model can be written as

$$P_{\text{open}} = \frac{1}{1 + BL(0)\exp\left(\frac{-QFV}{RT}\right)} \quad (1)$$

where $L(0)$ is the open-to-closed equilibrium constant in the absence of bound calcium at 0 mV and for the allosteric gating scheme, the definition of B can be simplified as in Eq. 2.

$$B = \left[\frac{1 + \frac{[Ca]}{K_c}}{1 + \frac{[Ca]}{K_o}}\right]^4 \quad (2)$$

Here K_C and K_O represent the calcium dissociation constants from the closed and open states, respectively. Because the gating charge Q did not vary significantly for the different types of channels (Q ranged from 1.28 to 1.59 for different recordings, with an average value of 1.43 e^-), it was assumed to be invariant with channel type as well as the calcium concentration that the channel was exposed to. The dependence of P_{open} on $[Ca^{2+}]$ as described by Eqs. 1 and 2 was fit by varying three parameters for each channel type; the closed state affinity (K_C), the open state affinity (K_O), and the equilibrium between the closed and open states with no calcium ions bound (C_0 and O_0) at 0 mV [$L(0)$]. The simultaneous optimization for K_C, K_O, and $L(0)$ was performed using the "fmins" routine in MATLAB 5.1 (The MathWorks, Natick, MA). Changing the starting values for the three parameters by as much as one order of magnitude did not affect the final result, indicating that the values signify a global minimum.

Deactivation kinetics

Deactivation time constants measured from tail currents were obtained at different membrane voltages and calcium concentrations. For a step change in voltage to the allosteric gating model (voltage-dependent MWC model), the open probability may be defined as an exponential process given as follows (Cox et al., 1997):

$$P_{open}(t) = \left[\frac{a}{a+b}\right]_\infty - \left(\left[\frac{a}{a+b}\right]_\infty - \left[\frac{a}{a+b}\right]_0\right)e^{-(a+b)t} \quad (3)$$

where

$$a = (a_0 f_{C0} + a_1 f_{C1} + a_2 f_{C2} + a_3 f_{C3} + a_4 f_{C4})$$
$$b = (b_0 f_{O0} + b_1 f_{O1} + b_2 f_{O2} + b_3 f_{O3} + b_4 f_{O4})$$

Here a_x and b_x represent vertical rates denoting closed-to-open and open-to-closed transitions, respectively, and f_{cx} and f_{ox} represent the fraction of closed or open channels occupying state x at any given calcium. The macroscopic time constant given by $(1/a + b)$ is determined by an average of all the vertical rate constants in the scheme weighted by the fraction of channels in each closed (a) or open (b) state.

The deactivation kinetics were fit with Eq. 3 for each of the four channel types using the MATLAB fmins routine also. For each channel type, values of K_C, K_O, and $L(0)$ were obtained from steady-state fits to the MWC model. Representing the backward rates b_x as a function of the forward rates a_x by assuming microscopic reversibility for each loop in the gating scheme reduced the number of free parameters.

$$b_x/a_x = c[L(0)]^x$$

where $c = K_O/K_C$ and x = number of calcium ions bound in that state (x = 1 to 4).

Also, a_x and b_x have an exponential dependence on voltage. The gating charges associated with a_x and b_x are q_f and q_b, respectively. For conservation of total charge, the sum of the two charges must equal the steady-state gating charge (Q) between open and closed states.

Simultaneous fits to channel deactivation kinetics were performed for two calcium concentrations (1 and 5 μM) and at least five different voltages for each calcium concentration. Using two calcium concentrations allowed us to span a larger set of voltages and yielded more reproducible fitting results. Initial fits revealed multiple minimum points with large error surfaces for the free parameters (a_x). This was overcome by reducing the number of free parameters. We applied an extra set of conditions as applied before by Cui et al., 1997. The forward transition rates (a_x) were made to increase for transitions between closed and open states with more calcium ions bound to them ($a_4 > a_3 > a_2 > a_1 > a_0$). Similarly, the backward rates (b_x) decreased for transitions between open and closed states with more calcium ions ($b_4 < b_3 < b_2 < b_1 < b_0$). In addition, the gating charges, q_f and q_b, were set to be invariant after first round fits (average values were used because there was little variability). Applying the extra set of conditions yielded robust fits with a single minimum irrespective of the starting point. The values of the free parameters (a_x) and the dependent parameters (b_x) are listed in Table 2.

The hair cell model

Calcium channel open probability, calcium current, and calcium concentration at the pore of the BK channel were determined according Wu et al. (1995). BK channel transitions were simulated using the allosteric gating model described previously (Cox et al., 1997). The horizontal transitions between closed-closed or open-open states are assumed to occur with the same rate. The rate constant for calcium binding is given by $r[Ca_i]$ where r is the diffusion limited rate for calcium binding to each subunit and is assumed to be $10^3\ \mu M^{-1}s^{-1}$ (Cui et al., 1997). The vertical closed-to-open and open-to-closed rate constants are given by a_x and b_x, respectively, where x denotes the number of calcium ions bound to the channel. The probability of the channel to be in any state p_i is given by the linear differential equation

$$\frac{dp_i}{dt} = \sum_{j=1, j\neq i}^{N} (p_j k_{ji} - p_i k_{ij}) \quad \text{for } i = 1 \text{ to N} \quad (4)$$

N is the total number of states ($N = 10$ for this kinetic scheme, closed states are numbered 1–5 and the open states are numbered 6–10) and k_{ij} is the rate constant from state i to state j. If there is no transition from state i to state j, then $k_{ij} = 0$. The probability of opening p_{BK} is then determined by the sum of the probabilities of being in any of the open states (6–10).

$$p_{BK} = \sum_{i=6}^{10} p_i \quad (5)$$

Assuming a linear current-voltage relationship, the unitary current (i_{BK}) flowing through a BK channel is

$$i_{BK} = (V - E_K)g_{BK} \quad (6)$$

where E_K is the reversal potential for potassium (−90 mV) and g_K is the unitary conductance (50 pS at 22°C). The total current carried by all the BK channels (N_{BK}) would then be

$$I_{BK} = N_{BK} i_{BK} \quad (7)$$

The following physical constants were used to perform hair cell simulations:

R = 8.315 J mol^{-1} K^{-1} (Universal Gas Constant)
F = 96 480 C mol^{-1} (Faraday's constant)
T = 295 K/313 K (Absolute temperature at 22°C/40°C)

A hair cell capacitance of C = 7.0 pF and a leak conductance of G_L = 2.5 nS were used. The leak current was assumed to vary linearly with membrane voltage given by

$$I_L = G_L(V_m - 0) \quad (8)$$

At the start of the simulation all calcium channel m gates were assumed to be in the closed state and all BK channels were at the C_0 state. The number of channels N_{BK} and the scaling factor S_F were varied as shown in Tables 3 and 4 for different types of hair cells. The membrane voltage was determined by solving the current-clamp Eq. 9.

$$I(t) = C\frac{dV}{dt} + I_{Ca} + I_K + I_L \tag{9}$$

The hair cell current I(t) followed a square waveform from I_{rest} to I_{pulse} and back to I_{rest} as shown in Figs. 5 and 6. The model was allowed to achieve equilibrium in the first 10 ms and then the desired current clamp protocol was applied. First, the calcium current was calculated. Then, using the linear differential equation approximation, calcium concentration was calculated near the BK channel. BK channel open probability was determined using the voltage-dependent MWC model as in Eq. 4. Finally, the current clamp equation (Eq. 9) was solved using an implicit-Euler method with a step-size of 10 μs. Voltage-clamp simulations for different types of BK channels were performed by simply adding the individual currents from each channel.

RESULTS

Fitting cloned BK channel currents to the allosteric (voltage-dependent MWC) gating model

The effect of β modulation on BK channel gating was determined by comparing the properties of α subunits expressed alone, with those coexpressed with β subunits. Fig. 2 shows fits to average steady-state open probabilities of α_0 (*A*) and $\alpha_0\beta$ (*B*) channels expressed in HEK293 cells as a function of voltage at different concentrations of calcium, calculated according to Eqs. 1 and 2. As described in Methods, these fits were achieved by simultaneous optimization for K_C, K_O, and $L(0)$ at all voltages and calcium concentrations. These constants were then used in a subsequent test of the relationship between the half activation voltage and calcium concentration.

By rearranging Eq. 1, the half activation voltage $V_{1/2}$ (where P_{open} is 0.5), may be written as a function of calcium concentration.

$$V_{1/2} = \frac{RT}{QF}\ln(L(0)B) \tag{10}$$

$L(0)$ and B are defined above where B depends upon the calcium concentration (Eq. 2). The ratio between K_O and K_C determined the slope of the curve that fits the $V_{1/2}$ versus $[Ca^{2+}]$ relationship and the value of $L(0)$ determined the vertical position of the curve. This relationship of $V_{1/2}$ versus calcium concentration was used to fit voltage-clamp data for α_0 and $\alpha_0\beta$ in Fig. 3 (*solid line*). The allosteric gating model (or voltage-dependent MWC model) fits the $V_{1/2}$ relationship better than did a simple two-state voltage dependent calcium binding process (*dotted line*) used earlier (Ramanathan et al., 2000).

Steady-state open probability functions for the splice variant α_{61} (Genbank #AF076268) and its combination with β, ($\alpha_{61}\beta$) were also fit with the allosteric gating model (parameters in Table 1). The values show that α_{61} had slightly higher calcium affinities (corresponding to lower concentrations) than did α_0. There was a larger reduction in both K_C and K_O upon addition of β subunits to either channel, indicating a tighter binding of calcium to both closed and open states. The open-state affinity was more affected by β addition. The $L(0)$ term (reflecting the intrinsic voltage-sensitivity of each channel) also varied among the four channel models, but here the differences were greatest when comparing splice variants, and were affected less by addition of β subunits to any one splice variant. The gating charge (Q = 1.43) was assigned to each model.

The macroscopic time constant given by $(1/a+b)$ is determined by an average of all the vertical rate constants in the scheme weighted by the fraction of channels in each closed (a) or open (b) state. Equation 3 was used to fit

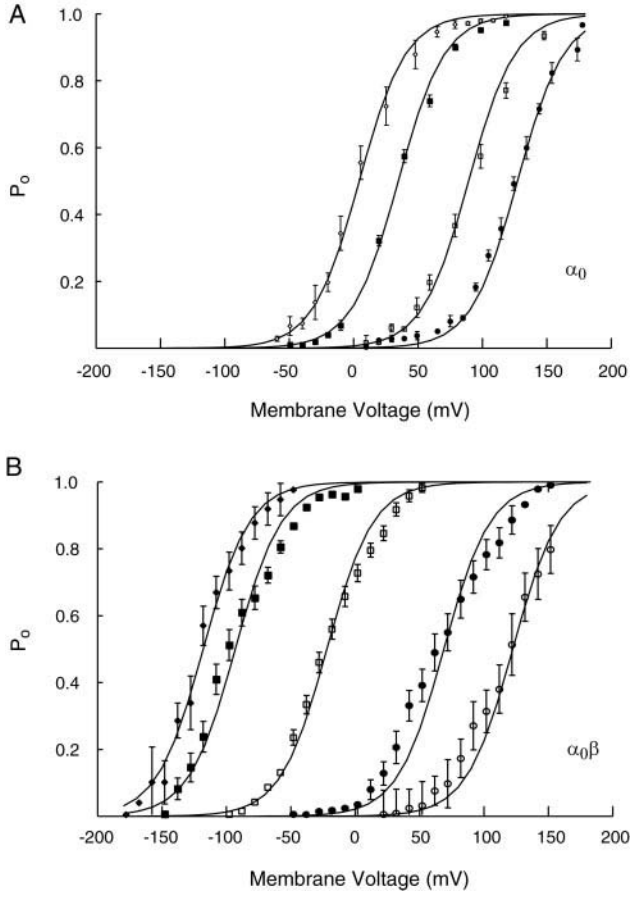

FIGURE 2 Voltage gated-MWC model fits to steady-state open probability of α_0 and $\alpha_0\beta$. (*A*) Channel open probability for α_0 expressed in HEK293 cells, determined from tail current amplitudes, is plotted as a function of membrane voltage for different cytoplasmic calcium concentrations (1.0, 2.0, 5.0, and 25.0 μM from right to left). The datapoints are fit with open probability functions defined for a voltage-dependent MWC scheme (*solid lines*) as defined by Eq. 1. (*B*) Fits for $\alpha_0\beta$ are performed as in *A*, for calcium concentrations of 0.2, 1.0, 5.0, 25.0, and 50.0 μM (from right to left). The gating charge Q was held constant at 1.43 e^- for all fits. Fits were performed simultaneously for all calcium concentrations and voltages for each channel type.

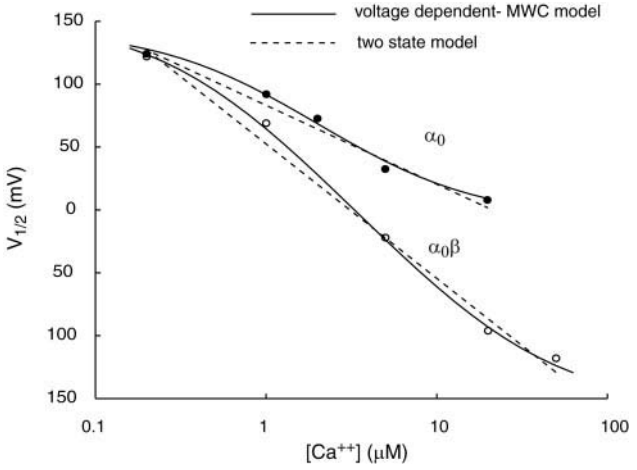

FIGURE 3 Voltage-dependent MWC model fits for the dependence of $V_{1/2}$ on calcium concentration. The $V_{1/2}$ vs. $[Ca^{2+}]$ relationship for α_0 and $\alpha_0\beta$ is fit with the voltage-dependent MWC scheme (*solid line*) using Eq. 10. The values of the parameters are listed in Table 1. The dotted line shows the fit provided by a simple two-state model (Ramanathan et al., 2000).

simultaneously deactivation time constants measured at calcium concentrations of 1 and 5 μM for α_0 and $\alpha_0\beta$ expressed in HEK293 cells (Fig. 4., *A* and *B*). Values of the kinetic parameters for those channels and from similar fits of the α_{61}, $\alpha_{61}\beta$ channels, are listed in Table 2 along with the gating charge. Transition rates were reduced, both by addition of β subunits and by insertion of the 61 aa exon, although the β subunit produced larger effects than did alternative splicing.

Constructing the model hair cells

With parameters for the channel models in hand we next incorporated these into an elementary model of chicken hair cells (Fig. 1 *B*) based on previous quantitative models of turtle hair cells (Wu et al., 1995). The basolateral membrane of the hair cell is thought to contain clusters of BK channels and calcium channels at distinct regions where transmitter release occurs (Roberts et al., 1990; Issa and Hudspeth, 1994; Martinez-Dunst et al., 1997). The total number of voltage-gated calcium channels per hair cell was set to be twice the total number of BK channels, and the open probability and dynamics of current through the calcium channels were based on experimental measurement from turtle

TABLE 1 Steady-state parameters for voltage dependent-MWC scheme

	α_0	$\alpha_0\beta$	α_{61}	$\alpha_{61}\beta$
K_C (μM)	35	25.4	25.4	20.8
K_O (μM)	1.18	0.58	1	0.6
$L(0)$	1766	1670	782	440
Q (e^-)	1.43	1.43	1.43	1.43

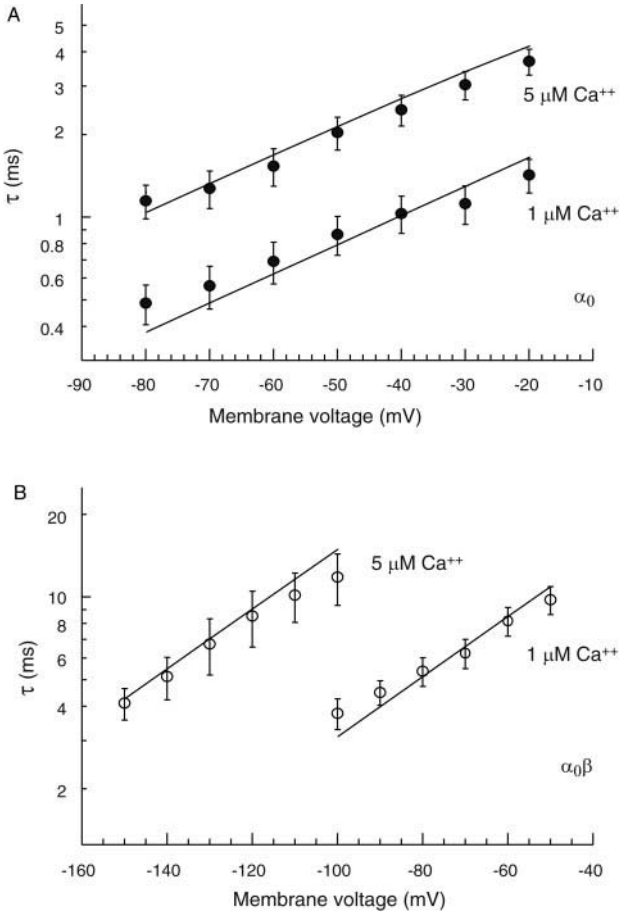

FIGURE 4 Channel deactivation time constant fit with a voltage-dependent MWC (allosteric) model. (*A*) Tail current deactivation time constants are plotted as a function of voltage for α_0 expressed in HEK293 cells and fit with model time constants by fitting the data points to the voltage-dependent MWC scheme (Eq. 3). The values of K_C, K_O, and $L(0)$ were the same as those used in fitting steady-state relationships (Table 1). The free parameters are listed in Table 2. (*B*) Voltage-dependent MWC scheme fit to the deactivation kinetics of $\alpha_0\beta$ as in (*A*).

(Art and Fettiplace, 1987), whose voltage-gated calcium channels are essentially identical to those of chickens (Zidanic and Fuchs, 1995). Although we mention that calcium channels and BK channels cluster at release sites, for the purpose of this model it is sufficient to assume that the calcium level near each BK channel is influenced by two nearby calcium channels. Indeed, each such BK channel is treated as an independent entity, gated solely by its attendant calcium channels.

A first order linear differential equation was used to describe calcium diffusion from an open calcium channel to a neighboring BK channel (Wu et al., 1995).

$$d[\mathrm{Ca}]/dt = 2S_F p_o(t) i_{Ca} - k_R[\mathrm{Ca}] \qquad (11)$$

S_F determines the calcium concentration achievable near a BK channel and reflects the buffering conditions and the distance between the BK channels and their closest calcium

TABLE 2 Kinetic rates and gating charge for α_0, $\alpha_0\beta$, α_{61}, and $\alpha_{61}\beta$

	α_0	$\alpha_0\beta$	α_{61}	$\alpha_{61}\beta$
a_0	0.45	0.10	0.30	0.40
a_1	9.8	2.3	2.8	4.13
a_2	137	29	42	32
a_3	1851	470	980	155
a_4	8140	2900	4946	2184
Q_f (e^-)	0.78	0.78	0.78	0.78
b_0	794.7	167.0	234.6	176.0
b_1	583.5	87.7	86.2	52.4
b_2	275.0	25.2	50.9	11.7
b_3	125.3	9.4	46.8	1.6
b_4	18.6	1.3	9.3	0.67
Q_b (e^-)	0.65	0.65	0.65	0.65

channels. k_R is the rate of calcium absorption by the ambient buffer. The ratio of S_F to k_R determines the available calcium at the pore of the BK channel. Resonance could be obtained for different values of S_F and k_R, but was sensitive to their ratio.

Fig. 5 shows responses of model hair cells operating at 22°C, each constructed with a single type of BK channel based on the properties of cloned, expressed α and β subunits. The panels are arranged in decreasing order of frequency. α_0, the channel with the most rapid kinetics generated a ringing frequency of 282 Hz and $\alpha_{61}\beta$, the slowest channel produced a hair cell that oscillated at 88 Hz. α_{61} and $\alpha_0\beta$ formed intermediate frequencies of 195 and 121 Hz, respectively. Thus, BK channel subunits cloned from the avian basilar papilla were sufficient to generate electrical tuning in a manner similar to that provided by native hair cell BK channels. Further, differences in the kinetics of those channels gave rise to different tuning frequencies.

One feature of this simulation departed from expectation; that was the resting potential of hair cells tuned to the lower frequencies, namely those generated by $\alpha_0\beta$ and $\alpha_{61}\beta$ channels. Both these model cells had resting potentials near −25 mV, compared to resting potentials between −40 and −60 mV in live hair cells. This difference may arise from the fact that other voltage-gated potassium channels, such as the inward rectifier, increase the total resting potassium conductance of living low frequency hair cells (Fuchs and Evans, 1990; Murrow, 1994; Holt and Eatock, 1995; Goodman and Art, 1996), but are absent from the model cells.

As for any resonance system, a hair cell's electrical resonance can be described by its fundamental resonant frequency F_0 and the quality of the resonance Q_{3dB}. The quality of resonance is equivalent to the sharpness of tuning, with a larger Q indicating sharper tuning. Higher quality resonances also have prolonged "ringing" responses to a transient stimulus, and so the Q can be derived from the time constant of decay of oscillations

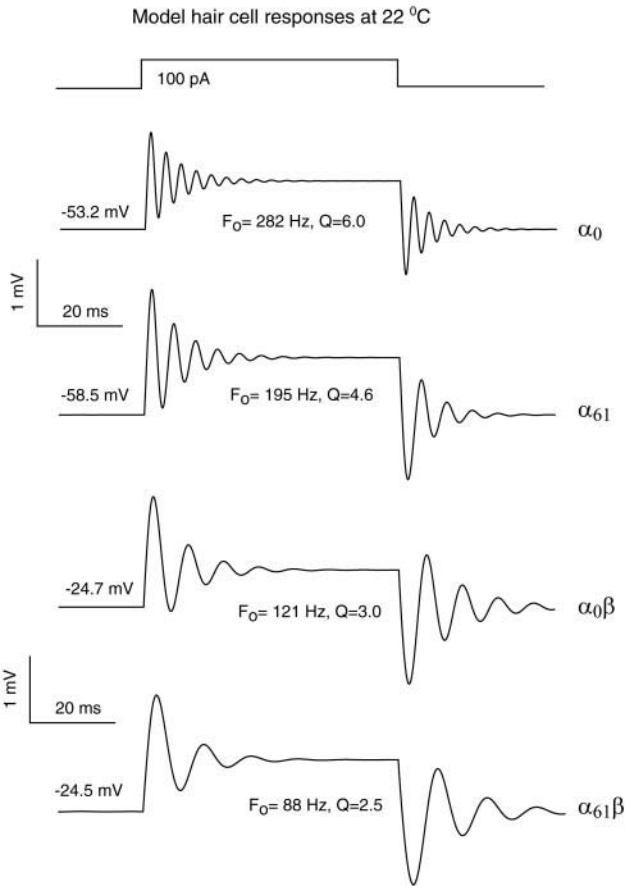

FIGURE 5 Electrical tuning of model hair cells expressing four types of BK channels. Model hair cells expressing 1of the 4 channel types were subject to current injection of 100 pA to excite electrical resonance. Channel numbers and model parameters were varied for each trial. Channels with faster kinetics (α_0 and α_{61}) were present in larger numbers whereas those with β subunits were present in smaller numbers (Wu et al., 1995). The four channels span a electrical tuning frequency range from 88 Hz to 282 Hz. The resonant frequency and the quality of tuning for positive current injection are shown below each trace. α_0 and α_{61} produced electrical resonance at resting hair cell voltages of ~−55 mV. Hair cells containing $\alpha_0\beta$ or $\alpha_{61}\beta$ resonated at resting potentials that were more depolarized (~−25 mV).

(τ) to such a transient stimulus (Crawford and Fettiplace, 1981; Wu et al., 1995).

$$Q_{3dB} = [(\pi F_0 \tau)^2 + 0.25]^{1/2} \quad (12)$$

As observed in experimental recordings from living hair cells, the Q_{3dB} of the model cells varied between 2.5 and

TABLE 3 Model parameters and resulting frequencies at 22°C

Channel type	α_0	α_{61}	$\alpha_0\beta$	$\alpha_{61}\beta$
N (# channels)	1200	800	500	400
S_F (μMs^{-1} pA^{-1})*10^6	16.5	15.0	2.0	1.5
K_R (ms^{-1})	40	40	40	40
F (Hz)	282	195	121	88
Q_{3dB} (quality factor)	6.0	4.6	3.0	2.5

TABLE 4 Model parameters and resulting frequencies at 40°C

Channel type	α_0	α_{61}	$\alpha_0\beta$	$\alpha_{61}\beta$
N (# channels)	3000	2400	1500	1500
S_F (μMs^{-1} pA^{-1})*10^6	68	45	16	14
K_R (ms^{-1})	80	80	80	80
F (Hz)	1133	788	424	307
Q_{3dB} (quality factor)	7.2	7.5	4.5	3.5

6.0. The parameters used in each model hair cell model and the resulting tuning are listed in Table 3.

Two parameters were preset for each hair cell model. The calcium extrusion rate K_R was 40 in all cases. The number of BK channels per hair cell (N) was set to replicate the relationship between tuning frequency and channel number found in electrically tuned turtle hair cells (Wu et al., 1995). We estimated the expected tuning frequency for each model from the time constant of decay of macroscopic currents through the cloned channel type that constituted that model (Ramanathan et al., 2000). An initial value for S_F was based on previous modeling studies of turtle hair cells (Wu et al., 1995) and then adjusted empirically in order to provide a quality of resonance (Q) between 2 and 11. Much lower or higher values of S_F did not result in voltage oscillations for each channel type.

Temperature effects on resonance

The preceding results were obtained at a temperature of 22°C, consistent with experimental studies of cloned channels in HEK293 cells and work on turtle hair cells. However, body temperature in birds such as the chicken is near 40°C, and both hair cell oscillation frequency (Fuchs and Evans, 1990), as well as the tuning frequency of afferent fibers (Schermuly and Klinke, 1985; Wu et al., 1995), have been shown to vary approximately twofold per 10°C temperature change. Thus, we applied temperature corrections to channel kinetics as well as other features of the model to determine tuning behavior at 40°C. These were:

1. Rate constants for BK and calcium channels were scaled by a factor of 7. BK channels in guinea pig urinary bladder myocytes had Q_{10} values near 3.0 for activation and deactivation rates (Markwardt and Isenberg, 1992). Q_{10} is defined as the increase in the rate for a 10-fold rise in temperature. Hence, for an 18°C rise in temperature, the new rates $R_{40°C} = R_{22°C} \cdot (Q10)^{1.8}$.

2. Single channel conductances of BK channels and calcium channels were doubled. Typical Q_{10} values for conductance are between 1.3 and 1.6 for most channels. Potassium channels in the axons of *Xenopus laevis* had Q_{10} values ~1.5 (Frankenhaeuser and Moore, 1963). BK channels in cultured rat muscle had a similar temperature dependence (Barrett et al., 1982).

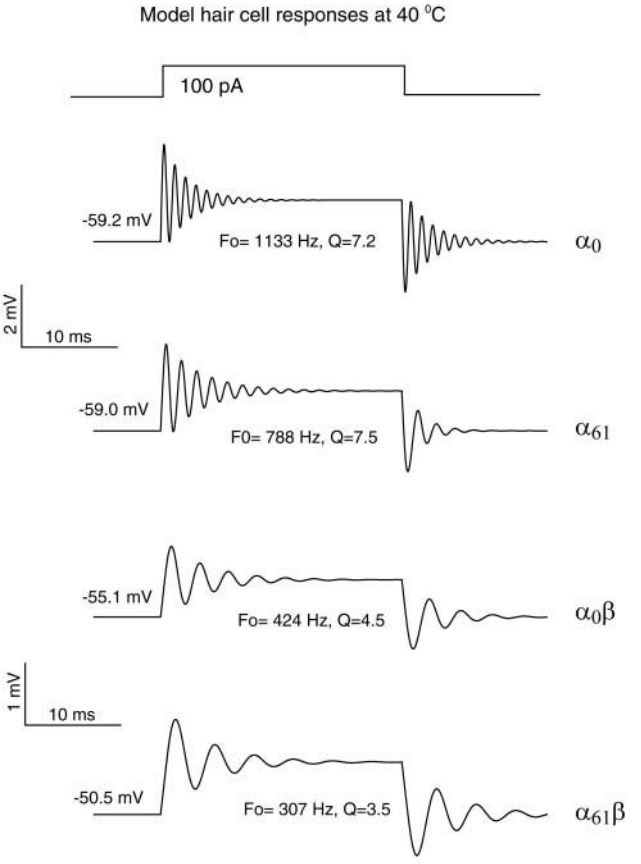

FIGURE 6 Model hair cell electrical tuning at chicken body temperature. When temperature corrections were made to simulate resonance at the body temperature of the chick (40°C), the frequencies increased almost fourfold spanning a range from 307 Hz to 1133 Hz. The resting membrane voltages were between −50 and −59 mV. The increase in temperature caused models containing β subunits to oscillate near hair cell resting potentials (cf. Fig. 5).

3. Channel numbers were increased two- to threefold. This is in formal agreement with voltage-clamp measurements which show that hair cells tuned to higher frequency have larger numbers of calcium and potassium channels (Martinez-Dunst et al., 1997; Art et al., 1987). In the models, higher channel numbers produced higher quality of resonance (Q_{3dB}). Increasing channel numbers by threefold produced quality factors between 3.0 and 8.0. Although using the smaller number of channels for the simulation of higher temperature did not change the resonant frequency significantly, the numbers were increased to preserve the quality factors, which were lower when the channel numbers were not increased. The parameters used for the increased body temperature of 40°C for electrical tuning simulations are listed in Table 4.

Using the new model parameters, simulations were performed to determine what oscillation frequencies these model hair cells would produce. Fig. 6 shows the results from the simulation of the same four channel types as in Fig.

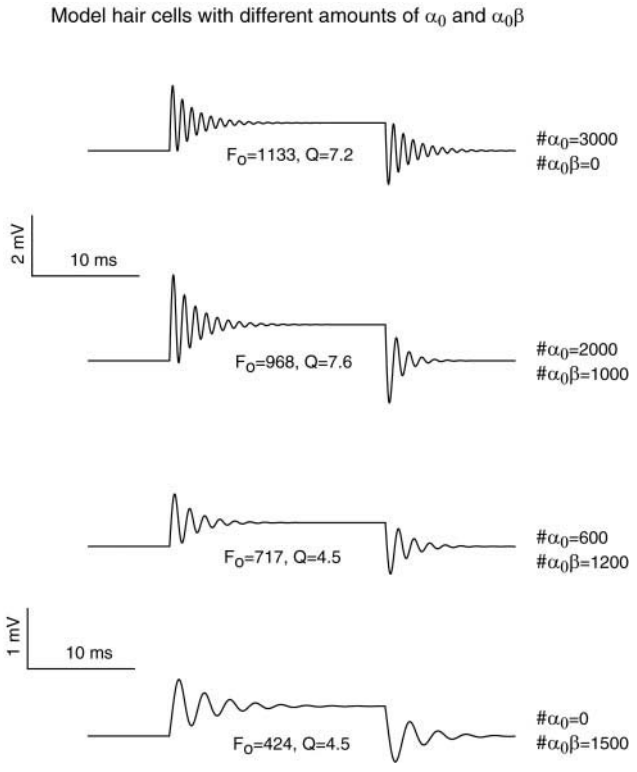

FIGURE 7 Channel titration to obtain intermediate frequencies in model hair cells. The effect of mixing two channel types in a model hair cell is examined. Different ratios of α_0 and $\alpha_0\beta$ are inserted in model hair cells, which are tested with a 100-pA current injection. Cells that express either α_0 or $\alpha_0\beta$ were the same as in Fig. 6. When the ratio of α_0:$\alpha_0\beta$ is 2:1, the tuning frequency was 968 Hz, and when the ratio was 1:2, the frequency was 717 Hz.

5. The frequencies have increased almost fourfold to span a range from 307 Hz to 1133 Hz. This increase in frequencies with temperature provides a Q_{10} value of 1.84, which is essentially that observed by Fuchs and Evans (1990) for chick hair cell electrical resonance frequencies and by Schermuly and Klinke (1985) for auditory nerve fiber tuning (Q_{10} = 2.0 in both cases). Hence, the temperature dependence of biophysical properties could be entirely responsible for the temperature dependence of tuning obtained by direct measurements from hair cells and auditory nerve fibers. Moreover, the resting hair cell potentials (−51 to −59 mV) were very near those observed in isolated chick hair cells (−40 to −60 mV), presumably as a result of the increase in potassium conductance.

β subunit titration

We have modeled four types of cloned channels that encode frequencies extending from 307 to 1133 Hz at 40°C. The next question was to test a method of channel expression that could result in a gradient of tuning along the tonotopically organized auditory epithelium. Both alternative splicing of α subunits and combination with β subunits alter the gating kinetics of the resulting channels. Only limited information is available on the tonotopic distribution of α splice variants in the chick (Navaratnam et al., 1997; Rosenblatt et al., 1997). However, we know from in situ hybridization experiments that there is a smooth gradient in β mRNA expression along the length of the basilar papilla (Ramanathan et al., 1999). Thus, we have used the model hair cells to ask whether β subunits might be titrated to alter BK channels kinetics and hair cell tuning. In particular, we have asked whether it is possible simply to mix together α-only and α-plus-β channels to produce hair cells with intermediate tuning. Intuitively, one would question whether the relatively large differences in kinetics between these channels could support the "homogeneous" behavior necessary for voltage oscillations.

We tested this idea using model cells with different ratios of α_0 and $\alpha_0\beta$ channels, operating at 40°C. Each BK channel was again assumed to obtain its calcium ions from two neighboring calcium channels. Hence, all BK channels would "see" the same amount of calcium for a given membrane potential. The total number of BK channels was varied so that lower frequency cells had fewer BK channels than their high frequency counterparts, corresponding to previous observation (Art et al., 1987; Fuchs et al., 1988). The total potassium current was obtained by multiplying the current through each BK channel by their respective numbers in the model cell. The responses of these model hair cells to current injections are shown in Fig. 7. Two conclusions can be drawn: 1) a hair cell expressing a mixture of channel types can oscillate with a single frequency and 2) its tuning frequency is intermediate to those produced by each channel type expressed on its own. Two intermediate combinations of α_0 and $\alpha_0\beta$ were tested in Fig. 7. The model hair cells oscillated at 968 Hz when one-third of the BK channels were of the $\alpha_0\beta$ form, and at 717 Hz when two-thirds were of the $\alpha_0\beta$ form. The resonance was similar to that of model hair cells containing a homogenous mixture of BK channels and produced exponentially decaying oscillations in membrane voltage that could be described by Eq. 13.

$$V = V_0\sin(2\pi F_0 t - \phi)\exp(-t/\tau) \qquad (13)$$

The resonant frequency F_0 and τ are as defined before (Eq. 12), V_0 is the maximum amplitude, and ϕ is the phase delay of the oscillations. This voltage response with a single characteristic frequency of a model hair cell containing a heterogeneous mixture of BK channels suggests three things. One, the population response of channels with widely different kinetics within a hair cell can be represented by a single kinetic parameter. Second, individual channels with intermediate kinetics are not mandatory for hair cells tuned to intermediate frequencies. A hair cell may express a complex mixture of BK channel subtypes with

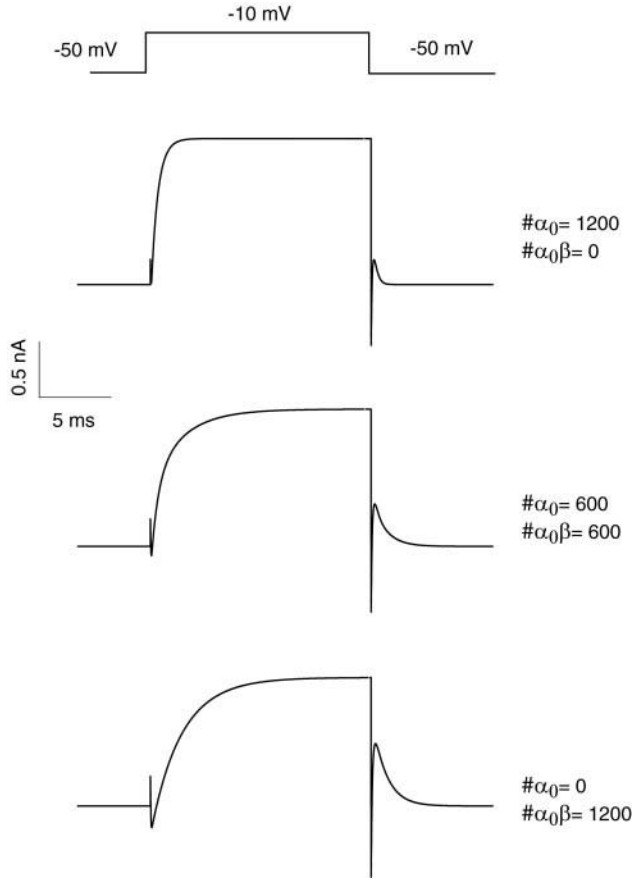

FIGURE 8 Voltage clamp responses of model hair cells. Model hair cells expressing different ratios of α_0 and $\alpha_0\beta$ were tested under voltage clamp. Their activation and deactivation kinetics were examined for multiple exponential components. The total number of BK channels and other model parameters were kept constant. Tail currents of hair cells containing equal amounts of α_0 and $\alpha_0\beta$ decayed with a time constant of 3.16 ms which was intermediate to the decay times of cells containing either α_0 (0.92 ms) or $\alpha_0\beta$ (3.84 ms) alone.

varying kinetic properties and yet have a unique resonance frequency that reflects an ensemble average of the properties of the constituent channels. Third and finally, hair cell-tuning can be produced by a functional gradient in β subunit expression.

Voltage-clamp responses

In the previous section it was shown that a model hair cell may contain channels with different kinetic properties, yet still produce a unimodal voltage resonance. This might arise by voltage feedback through membrane resistance and capacitance so that the membrane time constant serves to integrate or smooth multiple current kinetics. Thus, a further examination of model behavior was made under voltage clamp to examine current kinetics. Can multiple exponential components in current activation and deactivation be distinguished? We simulated the same models under voltage clamp mode and studied the kinetics of the "tail" currents, which in native hair cells have monoexponential kinetics whose time constants vary tonotopically. The calcium current was calculated at each time point from calcium channel open probability and fed back to the BK channel model to determine the potassium current. The resulting whole-cell current response is shown in the middle panel of Fig. 8 for a hair cell containing an equal number of α_0 and $\alpha_0\beta$. Activation and deactivation for this cell is intermediate between those of the α-only and all $\alpha\beta$ model cells (the upper and lower responses in Fig. 8).

The decay kinetics of tail currents were examined at higher resolution for a range of $\alpha\beta$ ratios (Fig. 9 *A*). Tail currents were fit with a single exponential function. The time constant of decay had a monotonic progression from fast to slow with increasing concentration of β subunits. This effect is summarized in Fig. 9, *B* and *C*. The hair cell with no β subunits had a relaxation rate of 1.12 ms^{-1} and the hair cell that has all $\alpha_0\beta$ channels relaxed with a rate of 0.26 ms^{-1}. Intermediate rates fell along an exponential function that varied from fastest to the slowest upon increasing fractional saturation with β subunits. The oscillation frequencies produced by each of these model cells is plotted in Fig. 9 *C* as a function of the fraction of BK channels that were β modified. This result agrees qualitatively with the finding that the expression of *slo*-β along the tonotopic axis of the cochlea can be described by a monotonically decreasing function with the highest levels at the (low frequency) apical region (Ramanathan et al., 1999).

DISCUSSION

A computational hair cell model based on the kinetic properties of cloned and expressed BK channel subunits was used to reconstruct electrical tuning. Graded variations in tuning frequency could be produced simply by altering the fraction of BK channels in each model cell that is modulated by accessory β subunits. These experiments were motivated by the observation that β subunit mRNA is expressed in a diminishing gradient from the low frequency end of the avian basilar papilla (Ramanathan et al., 1999).

Justification of the model

A variety of kinetic schemes have been used to describe BK channel gating, and these continue to evolve. Single BK channel recordings from skeletal muscle (Rothberg and Magleby, 1999; Nimigean and Magleby, 1999) and from transfected cells (Horrigan and Aldrich, 1999; Talukder and Aldrich, 2000) argue that the relatively simple allosteric model used here is an incomplete description of BK gating. These arguments include the observation of a multiplicity of open states, and evidence that channel opening can occur without charge movement in all four channel subunits.

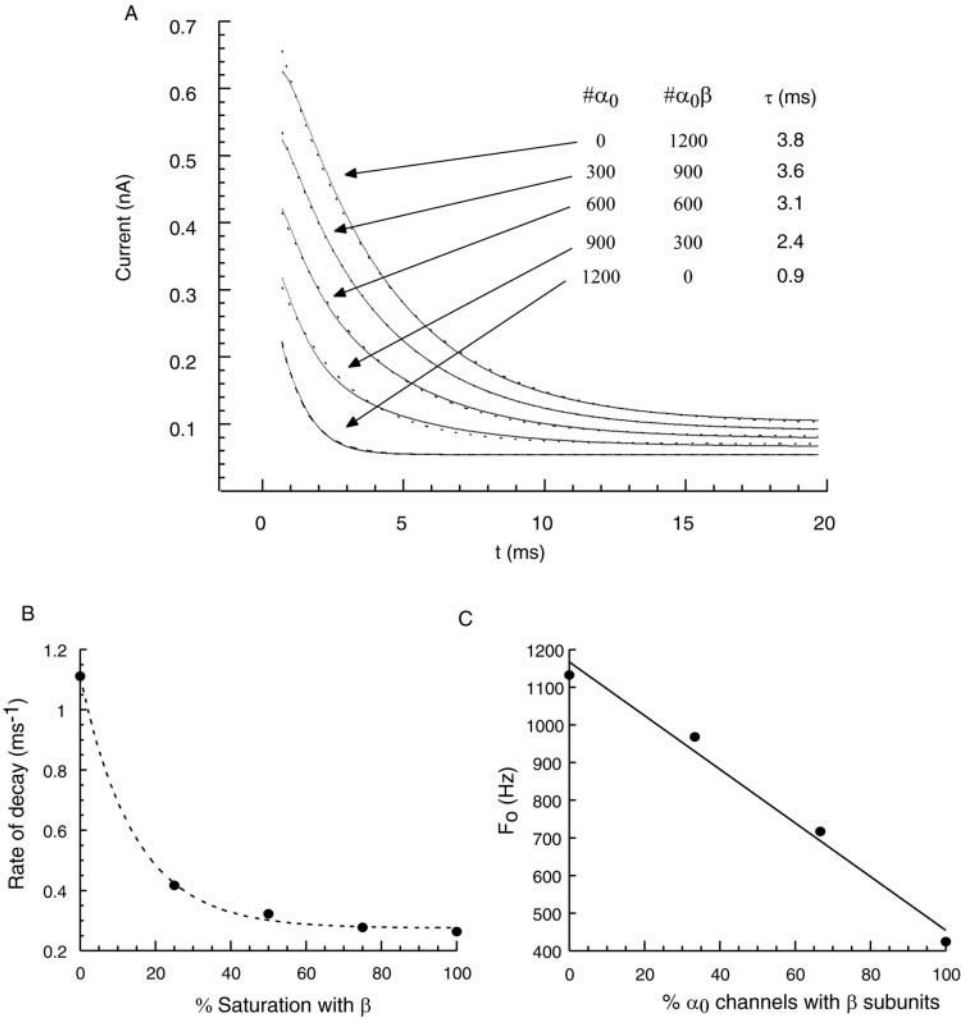

FIGURE 9 Tail currents of model hair cells in voltage clamp and effect of β titration on hair cell tuning frequencies. (*A*) Tail currents of model hair cells expressing different ratios of α_0 and $\alpha_0\beta$ were examined in isolation. For a total of 1200 BK channels, tail currents for different saturation levels with β subunits show that they can all be fit with a single exponential curve (*dashed lines*). The voltage command was the same for all ratios of channels (deactivation from -10 to -50 mV). Because $\alpha_0\beta$ channels had a higher affinity for calcium, they have a higher open probability under identical conditions of voltage and calcium and so a larger current is observed. The equation for monoexponential fits is given by $I = I_b + I_0\exp(-t/\tau)$, where I_b is the baseline current, I_0 is the maximum current amplitude, and τ is the time constant of decay. The goodness of fit was greater than 0.99 for all single exponential fits, equivalent to that obtained by fitting double exponential functions for the tail currents. (*B*) Rate of decay of tail currents (inverse of time constants from *A*) is plotted as a function of β saturation of the channels. The rates are fit with a relationship given by $r = r_b + r_0\exp(-f_b/b)$, where r_b is the rate of decay of 100% β saturated hair cell, r_0 is the difference between fastest and slowest rates, f_b is the fractional saturation with β subunits, and b is a fractional saturation analogous to a length constant. (*C*) Hair cell-tuning frequency plotted vs. fraction of α_0 channels combined with β subunits. A hair cell expressing only α_0 is tuned to 1133 Hz and addition of β subunits reduces the frequency proportionally until all the channels are β-bound and the frequency becomes 424 Hz. The data points were fit with a straight line given by $F_0 = m\beta_x + F_c$, where β_x is the fraction of total channels containing β subunits, m is the slope of the line, and F_c is the theoretical frequency when β subunits are absent.

Nonetheless, the relatively restricted allosteric kinetic scheme is adequate for a quantitative description of the macroscopic currents generated by the cloned channels in HEK293 cells. The parameters of those fits provided a practical method to construct the excitability of model hair cells. Although such a channel model may not serve for insights into the mechanisms of BK channel gating per se, it enables a quantitative assessment of the whole-cell integration of multiple channel types as intended here.

We have used quantitative models based on the properties of cloned BK channels to show that a gradient of tuning frequencies among hair cells could be generated by the blending of kinetically distinct channel types. This effort arose from a desire to test the sufficiency of cochlear gene products to reconstruct hair cell tuning, and from the observation that β subunit mRNA appears in a gradient along the tonotopic axis of the avian basilar papilla when visualized with in situ hybridization (Ramanathan et al., 1999). Such a

gradient in β expression was assumed to result in a heterogeneous population of BK channels in each hair cell, some fraction being "β-modified," the remainder not. Because modulation by β subunits slows BK gating kinetics at least 10-fold (Jones et al., 1999; Ramanathan et al., 2000), we wished to determine whether such a pool of BK channels with widely variant gating kinetics could generate a single well behaved electrical resonance in a model hair cell.

An alternative approach would have been to construct heterotetrameric BK channels in which a variable fraction of the four α subunits were modified by combination with β subunits. Such a mechanism seems intrinsically better suited for fine gradations in channel properties, as might be expected for generating a continuum in hair cell tuning. Indeed, such heteromeric channels were proposed as part of an earlier model of tuning in turtle hair cells (Wu and Fettiplace, 1996). However, present evidence argues against β modulation occurring by such graded combination. Studies of $\alpha\beta$ coexpression in *Xenopus* oocytes showed that the effect of β subunits was all-or-nothing, irrespective of the stoichiometry of injected cRNAs (Jones et al., 1999). Likewise, cotransfection of HEK293 cells with different ratios of cDNAs never resulted in current with multiple kinetic components (Ramanathan and Michael, unpublished). Nonetheless, these experimental approaches do not completely resolve this issue, and further study is required to define the stoichiometry of $\alpha\beta$ association. If the all-or-none modulatory effect of β subunits is confirmed, the present work demonstrates that such an interaction does not prevent β modulation from serving as a means to tune hair cell BK channels.

Implications of the model

The hair cell models have shown that the gating properties of cloned and heterologously expressed cochlear *slo* gene products are sufficient to generate electrical tuning. Furthermore, coexpression with β subunits lowers the resonant frequency for model hair cells containing any one α subunit splice variant. Also, previously published effects of temperature on channel gating and conductance were used to alter the model and to recapitulate the temperature dependence of tuning in hair cells and afferent fibers. Finally, when model hair cells were composed of mixtures of α-only and $\alpha\beta$ channels, monoexponential macroscopic current decays were generated, and intermediate tuning frequencies were produced. This unexpected blending of channel kinetics may reflect the combined effect of the β subunit on kinetics and the calcium/voltage sensitivity of the channels. For example, after a depolarizing voltage command, α-only channels, with lesser calcium and voltage sensitivities, will contribute at early times, whereas the more sensitive $\alpha\beta$ channels will dominate at later times. Thus, not only the open probability of each channel type, but also the ratio between them changes exponentially as calcium and voltage decay. These results predict that electrically tuned hair cells should possess distinct populations of BK channels with different calcium- and voltage-sensitivities, reflecting the presence or absence of modulatory β subunits. This was not revealed in the original studies on turtle hair cells (Wu et al., 1995) but warrants revisiting in the avian papilla from which these gene products were obtained. Finally, it should be emphasized that this modeling effort does not provide evidence to the all-or-none effect of β subunits on *slo*-α channels, nor does it eliminate other functional combinations. Thus, we can not conclude that other mechanisms such as subunit mixing do not also contribute to smooth gradients in electrical tuning frequencies along the basilar papilla.

Limitations of the model

As seen here, an expression gradient of β subunits by itself can not provide the entire range of electrical tuning. For example, the maximum change in tuning because of β modulation was from 1133 to 424 Hz for the α_0 splice variant, a factor of 2.67. Although the entire range of electrical tuning has not been established in chick, hearing spans a 100-fold range of frequencies, and electrical tuning by BK channels in turtle hair cells ranges ~50-fold, from 30 to 600 Hz (Wu et al., 1995). Additional range could be achieved by incorporating additional α splice variants; for example, $\alpha_{61}\beta$ has a resonant frequency of 307 Hz (at 40°C). Still other variants from the avian cochlea remain to be characterized (Navaratnam et al., 1997; Rosenblatt et al., 1997) and shorter α splice variants ($'4$, $-26'$) from turtle hair cells can have more rapid gating kinetics than those described here (Jones et al. 1999). Alternative splicing of the α subunit may provide the intrinsic kinetic variability in gating that is further exaggerated by β modulation. Additional variability might be conferred by other modulatory subunits. Four β genes have been described in mammals (Xia et al., 1999; Wallner et al., 1999; Brenner et al., 2000; Uebele et al., 2000), with the avian β possibly representing a fifth. Most of these β genes produce somewhat different effects on BK channel gating. Alternative splicing of one of these β genes provides still further variability (Uebele et al., 2000). Other modulatory subunits such as *Slob* (Schopperle et al., 1998) and *Slak* (Joiner et al., 1998), and modification by phosphorylation (Tian et al. 2001) or other processes also require examination in the context of electrical tuning.

With thanks to T. Michael for extensive discussion, and Dr. Hakim Hiel for β mRNA in situ hybridization results. Supported by grant #DC00276 from the National Institute of Deafness and Communication Disorders.

REFERENCES

Art, J. J., and R. Fettiplace. 1987. Variation of membrane properties in hair cells isolated from the turtle cochlea. *J. Physiol.* 385:207–242.

Art, J. J., Y. C. Wu, and R. Fettiplace. 1995. The calcium-activated potassium channels of turtle hair cells. *J. Gen. Physiol.* 105:49–72.

Ashmore, J. F. 1983. Frequency tuning in a frog vestibular organ. *Nature.* 304:536–538.

Barrett, J. N., K. L. Magleby, and B. S. Pallotta. 1982. Properties of single calcium-activated potassium channels in cultured rat muscle. *J. Physiol.* 331:211–330.

Brenner, R., T. J. Jegla, A. Wickenden, Y. Liu, and R. W. Aldrich. 2000. Cloning and functional characterization of novel large conductance calcium-activated potassium channel β subunits, hKCNMB3 and hKCNMB4. *J. Biol. Chem.* 275:6453–6461.

Cox, D. H., J. Cui, and R. W. Aldrich. 1997. Allosteric gating of a large conductance Ca^{2+}-activated K^+ channel. *J. Gen. Physiol.* 110:257–281.

Crawford, A. C., and R. Fettiplace. 1980. The frequency selectivity of auditory nerve fibres and hair cells in the cochlea of the turtle. *J. Physiol.* 306:79–125.

Crawford, A. C., and R. Fettiplace. 1981. An electrical tuning mechanism in turtle cochlear hair cells. *J. Physiol.* 312:377–412.

Cui, J., D. H. Cox, and R. W. Aldrich. 1997. Intrinsic voltage dependence and Ca^{2+} regulation of *mslo* large conductance Ca-activated K^+ channels. *J. Gen. Physiol.* 109:647–673.

Frankenhaeuser, B., and L. E. Moore. 1963. The effect of temperature on the sodium and potassium permeability changes in myelinated nerve fibres of *Xenopus laevis*. *J. Physiol.* 169:431–437.

Fuchs, P. A., and M. G. Evans. 1988. Voltage oscillations and ionic conductances in hair cells isolated from the alligator cochlea. *J. Comp. Physiol. A.* 164:151–163.

Fuchs, P. A., and M. G. Evans. 1990. Potassium currents in hair cells isolated from the cochlea of the chick. *J. Physiol.* 429:529–551.

Fuchs, P. A., T. Nagai, and M. G. Evans. 1988. Electrical tuning in hair cells isolated from the chick cochlea. *J. Neurosci.* 8:2460–2467.

Goodman, M. B., and J. J. Art. 1996. Positive feedback by a potassium-selective inward rectifier enhances tuning in vertebrate hair cells. *Biophys. J.* 71:430–442.

Holt, J. R., and R. A. Eatock. 1995. Inwardly rectifying currents of saccular hair cells from the leopard frog. *J. Neurophysiol.* 73:1484–1502.

Horrigan, F. T., and R. W. Aldrich. 1999. Allosteric voltage gating of potassium channels II. *Mslo* channel gating charge movement in the absence of Ca(2+). *J. Gen. Physiol.* 114:305–336.

Hudspeth, A. J., and R. S. Lewis. 1988a. Kinetic analysis of voltage- and ion-dependent conductances in saccular hair cells of the bull-frog *Rana catesbeiana*. *J. Physiol.* 400:237–274.

Hudspeth, A. J., and R. S. Lewis. 1988b. A model for electrical resonance and frequency tuning in saccular hair cells of the bull-frog *Rana catesbiana*. *J. Physiol.* 400:275–297.

Issa, N. P., and A. J. Hudspeth. 1994. Clustering of Ca^{2+} channels and $Ca(^{2+})$-activated K^+ channels at fluorescently labeled presynaptic active zones of hair cells. *Proc. Natl. Acad. Sci. U.S.A.* 91:7578–7582.

Jiang, G. J., M. Zidanic, R. L. Michaels, T. H. Michael, C. Griguer, and P. A. Fuchs. 1997. *Cslo* encodes calcium-activated potassium channels in the chick's cochlea. *Proc. R. Soc. Lond. B. Biol. Sci.* 264:731–737.

Joiner, W. J., M. D. Tang, L. Y. Wang, S. I. Dworetzky, C. G. Boissard, L. Gan, V. K. Gribkoff, and L. K. Kaczmarek. 1998. Formation of intermediate-conductance calcium-activated potassium channels by interaction of Slack and *slo* subunits. *Nat. Neurosci.* 1:462–469.

Jones, E. M., M. Gray-Keller, and R. Fettiplace. 1999. The role of Ca^{2+}-activated K^+ channel spliced variants in the tonotopic organization of the turtle cochlea. *J. Physiol.* 518:653–665.

Lewis, R. S., and A. J. Hudspeth. 1983. Voltage- and ion-dependent conductances in solitary vertebrate hair cells. *Nature.* 304:538–541.

Markwardt, F., and G. Isenberg. 1992. Gating of maxi K^+ channels studied by Ca^{2+} concentration jumps in excised inside-out multi-channel patches (myocytes from guinea pig urinary bladder). *J. Gen. Physiol.* 99:841–862.

Martinez-Dunst, C., R. L. Michaels, and P. A. Fuchs. 1997. Release sites and calcium channels in hair cells of the chick's cochlea. *J. Neurosci.* 17:9133–9144.

Murrow, B. W. 1994. Position-dependent expression of potassium currents by chick cochlear hair cells. *J. Physiol.* 480:247–259.

Navaratnam, D. S., T. J. Bell, T. D. Tu, E. L. Cohen, and J. C. Oberholtzer. 1997. Differential distribution of Ca^{2+}-activated K^+ channel splice variants among hair cells along the tonotopic axis of the chick cochlea. *Neuron.* 19:1077–1085.

Nimigean, C. M., and K. L. Magleby. 1999. The β subunit increases the Ca^{2+} sensitivity of large conductance Ca^{2+}-activated potassium channels by retaining the gating in the bursting states. *J. Gen. Physiol.* 113:425–440.

Oberst, C., R. Weiskirchen, M. Hartl, and K. Bister. 1997. Suppression in transformed avian fibroblasts of a gene (CO6) encoding a membrane protein related to mammalian potassium channel regulatory subunits. *Oncogene.* 14:1109–1116.

Ramanathan, K., T. H. Michael, and P. A. Fuchs. 2000. Beta subunits modulate alternatively spliced, large conductance, calcium-activated potassium channels of avian hair cells. *J. Neurosci.* 20:1675–1684.

Ramanathan, K., T. H. Michael, G. Jiang, H. Hiel, and P. A. Fuchs. 1999. A molecular mechanism for electrical tuning of cochlear hair cells. *Science.* 283:215–217.

Roberts, W. M., R. A. Jacobs, and A. J. Hudspeth. 1990. Colocalization of ion channels involved in frequency selectivity and synaptic transmission at presynaptic active zones of hair cells. *J. Neurosci.* 10:3664–3684.

Rosenblatt, K. P., Z. P. Sun, S. Heller, and A. J. Hudspeth. 1997. Distribution of Ca^{2+}-activated K^+ channel isoforms along the tonotopic gradient of the chicken's cochlea. *Neuron.* 19:1061–1075.

Rothberg, B. S., and K. L. Magleby. 1999. Gating kinetics of single large-conductance Ca^{2+}-activated K^+ channels in high Ca^{2+} suggest a two-tiered allosteric gating mechanism. *J. Gen. Physiol.* 114:93–124.

Schermuly, L., and R. Klinke. 1985. Change of characteristic frequency of pigeon primary auditory afferents with temperature. *J. Comp. Physiol.* 156:209–211.

Schopperle, W. M., M. H. Holmqvist, Y. Zhou, J. Wang, Z. Wang, L. C. Griffith, I. Keselman, F. Kusinitz, D. Dagan, and I. B. Levitan. 1998. *Slob*, a novel protein that interacts with the Slowpoke calcium-dependent potassium channel. *Neuron.* 20:565–573.

Sugihara, I., and T. Furukawa. 1989. Morphological and functional aspects of two different types of hair cells in the goldfish sacculus. *J. Neurophysiol.* 62:1330–1343.

Talukder, G., and R. W. Aldrich. 2000. Complex voltage-dependent behavior of single unliganded calcium-sensitive potassium channels. *Biophys. J.* 78:761–772.

Tian, L., R. R. Duncan, M. S. Hammond, L. S. Coghill, H. Wen, R. Rusinova, A. G. Clark, R. B. Levitan, and M. J. Shipston. 2001. Alternative splicing switches potassium channel sensitivity to protein phosphorylation. *J. Biol. Chem.* 276:7717–7720.

Uebele, V. N., A. Lagrutta, T. Wade, D. J. Figueroa, Y. Liu, E. McKenna, C. P. Austin, P. B. Bennett, and R. Swanson. 2000. Cloning and functional expression of two families of β-subunits of the large conductance calcium-activated K^+ channel. *J. Biol. Chem.* 275:23211–23218.

Wallner, M., P. Meera, and L. Toro. 1999. Molecular basis of fast inactivation in voltage and Ca^{2+}- activated K^+ channels: a transmembrane β-subunit homolog. *Proc. Natl. Acad. Sci. U.S.A.* 96:4137–4142.

Wu, Y. C., J. J. Art, M. B. Goodman, and R. Fettiplace. 1995. A kinetic description of the calcium-activated potassium channel and its application to electrical tuning of hair cells. *Prog. Biophys. Mol. Biol.* 63: 131–158.

Wu, Y. C., and R. Fettiplace. 1996. A developmental model for generating frequency maps in the reptilian and avian cochleas. *Biophys. J.* 70: 2557–2570.

Xia, X. M., J. P. Ding, and C. J. Lingle. 1999. Molecular basis for the inactivation of Ca^{2+} and voltage-dependent BK channels in adrenal chromaffin cells and rat insulinoma tumor cells. *J. Neurosci.* 19: 5255–5264.

Xie, J., and D. P. McCobb. 1998. Control of alternative splicing of potassium channels by stress hormones. *Science.* 280:443–446.

Zidanic, M., and P. A. Fuchs. 1995. Kinetic analysis of barium currents in chick cochlear hair cells. *Biophys. J.* 68:1323–1336.